2010 International Symposium on Nonlinear Theory and its Applications
NOLTA2010, Krakow, Poland, September 5-8, 2010

Synthesis of a spiking oscillator with a desired inter-spike-interval density

Tadashi Tsubone

The Department of Electrical Engineering, Nagaoka University of Technology,
1603–1 Kamitomioka–cho, Nagaoka–shi, Niigata, 940–2188 Japan, tsubone@vos.nagaokaut.ac.jp

Abstract—In this paper, we consider a design problem of a simple spiking oscillator with a desired inter-spike-interval (ISI) density. Our approach to the problem is based on a mapping procedure. The spiking oscillator behaves chaotic motions and generates various spike trains. It is important to study the relationship between a dynamic property of the oscillator and a static property on ISI density not only for scientific investigations, but also for engineering developments. We provide a simple spiking oscillator with piecewise constant vector fields. The dynamics of the system is governed by 1-D piecewise linear return map, therefore the rigorous analysis can be performed. We show an example of spiking oscillators with a conditional ISI density, its synthesis strategy is based on a probability density function of the 1-D return map.

1. Introduction

Chaotic spiking oscillators (abbr. CSO) have been studied in interesting works [1]-[3]. CSOs relate considerably to some spiking neuron neuron models [4]. The spiking neuron models have integrate-and-fire operation that generates a instantaneous pulse signal and reset a state variable instantaneously at the moment when the various reaches a switching threshold. Repeating the operations, CSOs generates a variety of spiking-trains. Study of the spiking-trains is important to develop some researches for information processing of the human brain, for pulse based communication systems and so on[5][6]. Also CSOs are included in hybrid dynamical systems with various nonlinear phenomena and its coupled systems can be developed into efficient applications of neural networks [7]. The analysis of spiking-trains and the simple circuit implementation of CSOs are important.

First, this paper presents a statistical analysis of the inter-spike-intervals (abbr. ISIs) generated from a CSO with piecewise constant vector field. The circuit consists mainly of two capacitors, two nonlinear voltage-controlled current sources and dependent impulsive switches. From the state space description, we derive the embedded return map which governs the qualitative behaviour of the system. The statical analysis of the return map results in the calculation of the invariant density. We derive the invariant density of the 1-D return map and show that the probability distribution of the ISIs for the CSO under consideration can be calculated from the invariant density of the return map. Second, we shows an example of synthesis procedure for a spiking oscillator with a conditional ISI probability density.

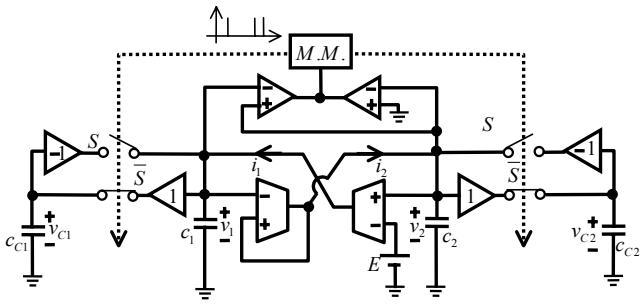

Figure 1: A chaotic spiking oscillator.

2. A chaotic spiking oscillator with piecewise-constant vector field

Figure 1 shows the circuit model of the simple chaotic spiking oscillator. The triangle labeled 1 (−1, respectively) is a linear amplifier with gain 1 (−1, respectively). The triangles labeled "+ −" are comparators. These amplifiers and comparators are realized by an operational amplifier with sufficiently large input impedance. Trapezoids are differential voltage-controlled transconductance amplifiers and their output currents are i_1 and i_2, respectively. They are characterised by

$$\begin{gathered} i_1 = I_a \cdot \mathrm{sgn}(v_2 - E), \\ i_2 = I_a \cdot \mathrm{sgn}(v_2 - v_1), \\ \left(\mathrm{sgn}(x) = \begin{cases} 1 & \text{for } x \geq 0, \\ -1 & \text{for } x < 0. \end{cases}\right) \end{gathered} \tag{1}$$

where v_1 and v_2 are voltages across the capacitors C_1 and C_2, respectively. I_a is constant which is controlled by a bias current of transconductance amplifiers. Connecting two capacitors to both output terminals of the

transconductance amplifiers, we obtain a two dimensional nonlinear system. When S is opened, the circuit dynamics is described by

$$\begin{aligned} \dot{x} &= \alpha \cdot \mathrm{sgn}(y-1), \\ \dot{y} &= \alpha \cdot \mathrm{sgn}(y-ax), \end{aligned} \tag{2}$$

where "$\cdot$" represents the derivative of τ, α is a constant value and the following dimensionless variables and parameters are used.

$$\begin{aligned} \tau = \frac{I_0}{C_2 E}t, \quad x = \frac{C_1}{C_2 E}v_1, \quad y = \frac{1}{E}v_2, \\ a = \frac{C_2}{C_1}, \quad \alpha = \frac{I_a}{I_0} > 0, \end{aligned} \tag{3}$$

where I_0 is a virtual constant current for normalizing. Here, we assume the following parameter condition:

$$a > \frac{\sqrt{2}+1}{\sqrt{2}-1}. \tag{4}$$

In this parameter range, Equation (2) has unstable rect-spiral trajectories as shown in Fig. 2. The trajectory on the phase space moves around the singular point $(\frac{1}{a}, 1)$ divergently and it must reach to the half line $l_{Th} = \{(x,y)|y = ax, y < 0\}$ as shown in the left figure of Fig. 2.

In this circuit in Fig. 1, $M.M.$ is a monostable multivibrator which outputs pulse signals to close the switch S and to open $\bar{S}$ instantaneously. Two comparators detect the impulsive switching condition. If $v_2 \le v_1$ or $v_2 \ge 0$, the switch S is opened and $\bar{S}$ is closed. For the meantime, the voltage v_1 and v_2 is stored to C_{C1} and C_{C2}, respectively. If $v_2 > v_1$ and $v_2 < 0$, then $M.M.$ is triggered by the pair of comparators, and the switch S is closed and $\bar{S}$ is opened instantaneously. At that time, the voltage v_1 and v_2 is reset instantaneously to the inverse voltage $-v_1$ and $-v_2$, respectively. that is,

$$\begin{aligned} [v_1(t^+), v_2(t^+)]^T = [-v_1(t), -v_2(t)]^T \\ \text{for } v_2(t) > v_1(t) \text{ and } v_2(t) < 0, \end{aligned} \tag{5}$$

where $t^+ \equiv \lim_{\varepsilon \to 0}\{t + \varepsilon\}$.

Because the parameter condition (4), the trajectory must reach $l_v \equiv \{(v_1, v_2)|v_2 = v_1, v_2 < 0\}$ when the switchings occur. Namely, the normalized trajectory must hit l_{Th}, and jumps from $(x(T_n), y(T_n))$ to $(-x(T_n^+), -y(T_n^+))$ as shown in the left figure of Fig. 2, where T_n is the n-th switching moments.

Consequently, Eqn. (2) and (5) with the condition (4) are transformed into

$$\begin{aligned} &\begin{cases} \dot{x} = \alpha \cdot \mathrm{sgn}(y-1), \\ \dot{y} = \alpha \cdot \mathrm{sgn}(y-ax), \end{cases} \quad \text{for } S = \text{off}, \\ &[x(\tau^+), y(\tau^+)]^T = [-x(\tau), -y(\tau)]^T \\ &\qquad \text{for } y(\tau) > a \cdot x(\tau) \text{ and } y(\tau) < 0, \\ &\qquad (a > \frac{\sqrt{2}+1}{\sqrt{2}-1}). \end{aligned} \tag{6}$$

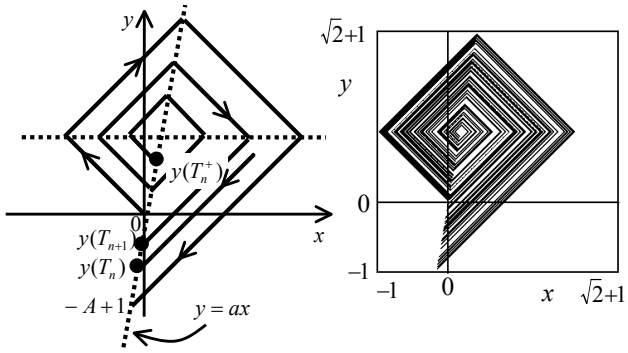

Figure 2: Behavior of Trajectories on the phase space and a typical chaos attractor. ($a \simeq 5.84$)

Now the system is characterized by only two parameters a and α. The right figure of Fig. 2 shows a typical chaotic attractor with $a \simeq 5.84$.

The transconductances are implemented by OTAs (LM13700). Realization procedure of differential voltage-controlled transconductance amplifiers by using OTAs can be found in literature [8]. The monostable multivibrator, the comparators and the analog switches are implemented by IC package of 4538, LM339 and LF398, respectively.

3. Embedded return map

The exact piecewise solution of Eqn. (6) for S =off can be depicted. Here, let us focus on a trajectory starting from origin at $\tau = 0$ (see Fig. 2). The trajectory rotates divergently around the singular point $(\frac{1}{a}, 1)$ and reaches the switching threshold. A $y-$coordinate of the reaching point is obtained as $-(\frac{a+1}{a-1})^2 + 1$. Here we define $A \equiv (\frac{a+1}{a-1})^2 > 1$ and $l \equiv \{(x,y)| -1 < y < 0, y = ax\}$. And we consider the case of $-A + 1 > -1$, that is, the minimum value of y is grater than -1. In this case, the trajectory starting from l must jumps instantaneously to the symmetric point of the origin, the trajectory rotates $k-$times $(k = 1, 2, 3, \cdots)$ around the singular point and it must return to l. We henceforth consider the following parameter range with (4):

$$1 < A \le 2. \tag{7}$$

If we choice l as Poincaré-section, we can define one dimensional return map f from l to itself. Letting $(x(T_n), y(T_n))$ be the starting point, $(x(T_{n+1}), y(T_{n+1}))$ be the return point as shown in left figure of Fig. 2. And letting any points on l be represented by its y-coordinate, f is defined by

$$f : l \mapsto l, \quad y_{n+1} = f(y_n), \tag{8}$$

where we rewrite $y_n = y(T_n)$.

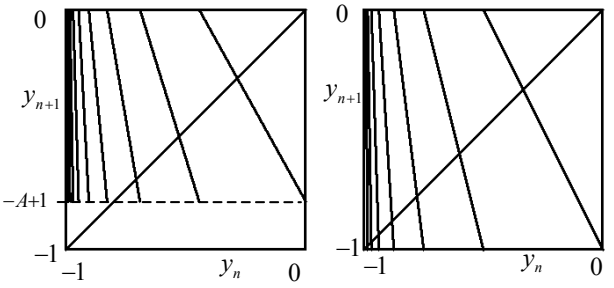

Figure 3: Chaotic return maps. (left: $A = 1.8(a \simeq 6.85)$, right: $A \to 2(a \simeq 5.84)$).

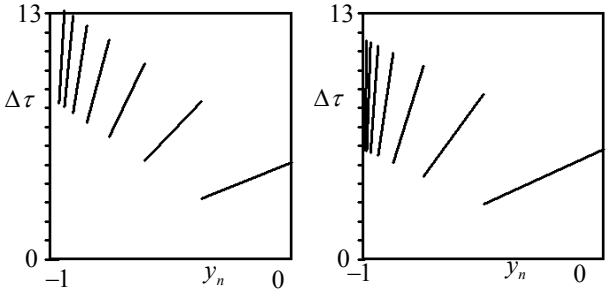

Figure 4: Relationship function ΔT between y and ISI. ($\alpha = 1$, left: $A = 1.6(a \simeq 8.55)$, right: $A \to 2(a \simeq 5.84)$).

By using piecewise-constant trajectories and linear algebraic procedure, we obtain an explicit expression for the function f:

$$f(y_n) = \begin{cases} -A(y_n+1)+1 \\ \quad \text{for } \frac{1}{A} - 1 < y_n \le 0, \\ -A^2(y_n+1)+1 \\ \quad \text{for } \frac{1}{A^2} - 1 < y_n \le \frac{1}{A} - 1, \\ \quad \vdots \\ -A^k(y_n+1)+1 \\ \quad \text{for } \frac{1}{A^k} - 1 < y_n \le \frac{1}{A^{k-1}} - 1, \\ \quad \vdots \\ \quad (k = 1, 2, 3, \cdots), \end{cases} \tag{9}$$

where each borders of the piecewise maps, $Th_k = \frac{1}{A^k} - 1$, are derived by solving $0 = -A^k(Th_k + 1) + 1$. Note that the return map f dose not depend on a parameter α. Typical map f are shown in Fig. 4. In this figure, k-th branch from the right corresponds to a trajectory with a k turn spiral on the phase space.

Here, we give the proof for chaos generation of this system. From condition (7), $|\frac{\partial f}{\partial x_n}| > 1$ is satisfied without discontinuous points and $f(l) \subset l$ is obvious, hence f exhibits chaos. In practice, if $1 < A < 4$ is satisfied, the system (6) behaves chaos rigorously. This paper omits the proof but it is easy in a similar way to [8].

4. Probability density of the inter-spike intervals

First, we derive the relationship function $\Delta T(y)$ between the inter-spike intervals $\Delta\tau$ and the state $y(T_n)$ at the moment when a spiking occurs. If the trajectory hits the threshold l at $\tau = T_n$, a spiking occurs and the time interval until next spiking is determined uniquely by $y(T_n)$. By using return map (8) and linear algebraic procedure, we obtain the expression for the function $\Delta T(y)$.

$$\Delta\tau = \Delta T(y) = \begin{cases} \frac{1}{\alpha}(1+y)(1+\sqrt{A})^2 \\ \quad \text{for } \frac{1}{A} - 1 < y_n \le 0, \\ \frac{1}{\alpha}(1+y)(1+\sqrt{A})^2(1+A) \\ \quad \text{for } \frac{1}{A^2} - 1 < y_n \le \frac{1}{A} - 1, \\ \quad \vdots \\ \frac{1}{\alpha}(1+y)(1+\sqrt{A})^2 \sum_{j=0}^{k-1} A^j \\ \quad \text{for } \frac{1}{A^k} - 1 < y_n \le \frac{1}{A^{k-1}} - 1, \\ \quad \vdots \\ \quad (k = 1, 2, 3, \cdots), \end{cases} \tag{10}$$

The examples of function ΔT is depicted in Fig. 4.

Second, we consider an invariant measure of the return map f. In order to derive the invariant measure, Frobenius-Perron operator P is well known to be useful. For the non-invertible map $f(y)$, its invariant measure can be obtained as the steady state of the iteration $f_{k+1}(y) = Pf_k(y)$ [9]. Here, we fix the parameter A to 2 for simplicity. In this case, the invariant measure $INV(y)$ of return map f must be uniform.

$$INV(y) = 1, \quad y \in [-1, 0] \tag{11}$$

Finally, using the invariant measure of return map $INV(y)$ and the relationship function ΔT, we can obtain directly the probability density function of ISI $d(\Delta\tau)$.

$$d(\Delta\tau) = \int_{-1}^{0} \left(\frac{\partial \Delta T(y)}{\partial y} \right)^{-1} \delta(y - y_T) INV(y) dy, \tag{12}$$

where y_T is the value such as $\Delta\tau = \Delta T(y_T)$, namely,

$$y_T = \Delta T^{-1}(\Delta\tau), \tag{13}$$

where ΔT^{-1} represents a inverse function of ΔT. The probability density function of ISI $d(\Delta\tau)$ with a parameter $a \simeq 5.84$ and $\alpha = 1$ is as shown in Fig. 5.

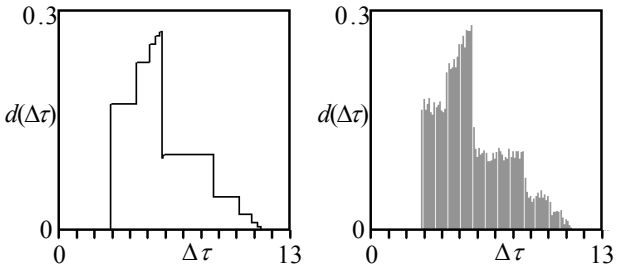

Figure 5: Probability density function of ISI. ($\alpha = 1$, $A = 2(a \simeq 5.84)$, left: theoretical, right: numerical.

The right figure of Fig. 5 shows histograms obtained by 100,000 sampled data of a numerical simulation.

5. Synthesis of a spiking oscillator with a conditional ISI density

In this section, we provide an example of synthesis approach to realize a spiking oscillator with a desired probability density of ISI. Here, we show the procedure to realize uniform density of ISI by controlling the relationship function ΔT.

We consider the α is a time variant parameter such as

$$\alpha = \begin{cases} \alpha_v & \text{for} \quad T_n \le \tau < T_n + \tau_\alpha, \\ 1 & \text{otherwise}, \end{cases} \tag{14}$$

where T_n is the n-th switching moments, τ_α is a suitable constant delay-time and

$$\alpha_v = 1 - \frac{1}{\tau_\alpha} \frac{(1+\sqrt{A})^2}{1-A} (y(T_n^+) - 1). \tag{15}$$

In this case, the relationship function ΔT changes as shown in Fig. 6, but the return map f is same to the case of constant α. From these the function and the return map, we obtain a uniform density of ISI as shown in Fig. 7.

6. conclusion

We considered a design problem of a simple spiking oscillator with a desired inter-spike-interval (ISI) density. Future subjects are a verification by experimental systems and an approach for generalisation.

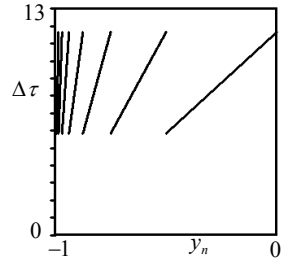

Figure 6: Relationship function ΔT between y and ISI on controlled system, ($A = 2(a \simeq 5.84)$).

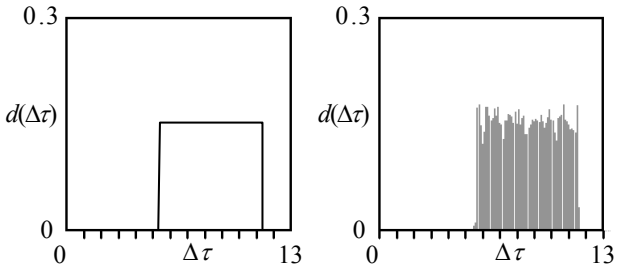

Figure 7: Probability density function of ISI (controlled). ($A = 2(a \simeq 5.84)$, left: theoretical, right: numerical.

References

[1] K.Mitsubori and T.Saito, "Dependent switched capacitor chaos generator and its synchronization, "IEEE Trans. Circuit Syst. I, 44, 12, pp.1122-1128 (1997).

[2] H. Nakano and T. Saito, "Grouping synchronization in a pulse-coupled network of chaotic spiking oscillators, "IEEE Trans. Neural Networks, 15, 5, pp. 1018-1026 (2004).

[3] Y. Takahashi, H. Nakano and T.Saito, "A simple hyperchaos generator based on impulsive switching," IEEE Trans. CAS-II, vol. 51, no. 9, pp. 468-472, (1998).

[4] Izhikevich, "Dynamical systems in neuroscience, " MIT Press, (2006).

[5] D. Laney, G.M. Maggio, F. Lehmann and L. Larson, "Multiple access for UWB impulse radio with pseudo-chaotic time hopping," IEEE J-SAC, vol. 20, no. 9, pp. 1692-1700, (2002).

[6] H. Torikai and T. Nishigami, "Response of a chaotic spiking neuron to various periodic inputs and its potential applications," IEICE Trans. Fundamentals, Vol. E92-A, No. 8, pp.2053-2060 (2009)

[7] H. Nakano and T. Saito, "Basic dynamics from an integrate-and-fire chaotic circuits with a periodic input," IEICE Trans. Fundamentals, Vol. E84-A, No. 5, pp.1293-1300 (2001).

[8] T. Tsubone and T. Saito, "Manifold piecewise constant systems and chaos," IEICE Trans. Fundamentals, vol. E82-A, no. 8, pp.1619–1626, (1999).

[9] A. Lasota and M. C. Mackey, "Chaos, Fractals, and Noise" Springer-Verlag, (1994).